

# Nanoscale

Accepted Manuscript



This is an *Accepted Manuscript*, which has been through the Royal Society of Chemistry peer review process and has been accepted for publication.

*Accepted Manuscripts* are published online shortly after acceptance, before technical editing, formatting and proof reading. Using this free service, authors can make their results available to the community, in citable form, before we publish the edited article. We will replace this *Accepted Manuscript* with the edited and formatted *Advance Article* as soon as it is available.

You can find more information about *Accepted Manuscripts* in the [Information for Authors](#).

Please note that technical editing may introduce minor changes to the text and/or graphics, which may alter content. The journal's standard [Terms & Conditions](#) and the [Ethical guidelines](#) still apply. In no event shall the Royal Society of Chemistry be held responsible for any errors or omissions in this *Accepted Manuscript* or any consequences arising from the use of any information it contains.

# Mitochondria-acting Hexokinase II Peptide Carried by Short-length Carbon Nanotubes with Increased Cellular Uptake, Endosomal Evasion, and Enhanced Bioactivity Against Cancer Cells

Cite this: DOI: 10.1039/x0xx00000x

Received 00th January 2012,  
Accepted 00th January 2012

DOI: 10.1039/x0xx00000x

www.rsc.org/

Sia Lee Yoong,<sup>a</sup> Wei Liang Lau,<sup>b</sup> Ang Yu Liu,<sup>b</sup> D'Arcy Prendergast,<sup>b</sup> Han Kiat Ho,<sup>b</sup> Victor Chun Kong Yu,<sup>ab</sup> Chengkuo Lee,<sup>c</sup> Wee Han Ang,<sup>\*ad</sup> and Giorgia Pastorin<sup>\*abe</sup>

Type II hexokinase (HKII) has emerged as viable therapeutic target due to its involvement in metabolic reprogramming and also apoptosis prevention. Peptide derived from the fifteen amino acid sequence at the HKII N-terminal region [HKII(pep)], can compete with endogenous proteins for binding on mitochondria and trigger apoptosis. However, this peptide is not cell-permeable. In this study, multi-walled carbon nanotubes (MWCNTs) were used to effectively deliver HKII(pep) across cellular barriers without compromising their bioactivity. The peptide was conjugated on either oxidized MWCNTs or 2,2'-(ethylenedioxy)bis(ethylamine)-functionalized MWCNTs, yielding MWCNT-HKII(pep) and MWCNT-TEG-HKII(pep), respectively. Both conjugates were shown to be internalized by breast cancer MCF-7 cells using confocal microscopy. Moreover, these nanoconjugates seemed to have escaped from endosome and be in vicinity of mitochondria. WST-1 cytotoxicity assay conducted on MCF-7 and colon carcinoma HCT116 cells revealed that MWCNT-peptide conjugates were significantly more effective in curbing cancer cell growth compared to a commercially available cell permeable HKII fusion peptide. In addition, both nanoconjugates displayed enhanced ability in eliciting apoptosis and depleting ATP level in HCT116 cells compared to mere HKII peptide. Importantly, hexokinase II release from mitochondria was demonstrated in MWCNT-HKII(pep) and MWCNT-TEG-HKII(pep) treated cells, highlighting that HKII(pep) structure and bioactivity was not compromised after covalent conjugation to MWCNTs.

## 1 Introduction

Hexokinase is an enzyme that phosphorylates glucose in an ATP-dependent manner and this commences the first committed step in glucose metabolism.<sup>1</sup> Among the four isozymes, only HKII possesses catalytically active N- and C-terminal halves. HKII binds onto the outer mitochondrial membrane (OMM) *via* its hydrophobic N-terminal region.<sup>2</sup> Voltage dependent anion channel (VDAC, also called porin), which forms the major channel for the exchange of metabolites and ions between mitochondria and other cellular compartments, was identified to be the protein interacting with HKII on the OMM.<sup>3</sup>

HKII is abundantly found in embryonic tissues and to a lesser extent in certain adult tissues, such as adipose, skeletal

muscles, and cardiac muscles.<sup>1</sup> Intriguingly, malignant tumours (lung cancer, breast cancer, colon cancer, etc.) exhibiting high glycolytic phenotype express higher levels (>100-fold) of HKII compared to normal cells.<sup>4,5</sup> In such tumours, mitochondrial HKII activity is also elevated.<sup>6</sup> As a result, these cells are able to survive and grow better in an oxygen-deprived environment inflicted by neoplastic mass accrual.<sup>7</sup>

HKII engages with four other partner proteins in aggravating the production of glucose-6-phosphate, which not only serves as precursor of glycolysis but also functions as intermediate for biosyntheses necessary for cancer cell proliferation. The four partner proteins include plasma membrane glucose transporter, VDAC, adenine nucleotide translocase (ANT) and ATP synthase at the inner mitochondrial membrane (IMM). Apart from that, HKII association with

VDAC has been shown to ingeniously desensitize tumour cells from cell death activation. It prevents proapoptotic Bcl-2 family members such as Bax and Bak from binding to mitochondria and this maintains mitochondrial integrity.<sup>8</sup> Targeted disruption of this association strongly induces cytochrome *c* release from mitochondria and apoptosis.<sup>9</sup>

Collectively, HKII represents a valuable therapeutic target for cancer therapy given its high expression level in cancer cells and engagement in the development of malignancy.<sup>1</sup> Compounds such as 3-bromopyruvate, clotrimazole and methyl jasmonate have been investigated *in vitro* and *in vivo* over the past years for their anti-cancer properties *via* inhibition of HKII binding to mitochondria.<sup>10</sup> Since these small molecule compounds can also trigger other cytotoxic mechanisms, the contribution of HKII inhibition in their cytotoxicity remains debatable.<sup>11-13</sup> Peptides corresponding to the N-terminal fifteen amino acids of HKII [HKII(pep)] have thus been employed as selective dissociating agents for HKII binding on mitochondria to elicit apoptosis.<sup>8,9,14,15</sup> Being impermeable to cell, they are generally conjugated to an internalization peptide sequence, often known as cell penetrating peptide (CPP), such as HIV-1 TAT or Drosophila Antennapedia, to facilitate cellular uptake. However, conjugation with CPP is unavoidably challenged by possible degradation (both extracellular and intracellular)<sup>16</sup> and endosomal entrapment.<sup>17</sup>

Nanocarriers have been employed to shield peptide against rapid peptidolysis and to selectively deliver them to cells *via* “passive” accumulation through the Enhanced Permeability and Retention (EPR) effect or “active” targeting by molecular recognition to designated sites.<sup>18,19</sup> Carbon nanotubes (CNTs) have emerged as a highly attractive nanodelivery system for several reasons. Firstly, their high ratio of length to diameter (aspect ratio) allows cellular entry *via* transmembrane penetration,<sup>20</sup> therefore bypassing endosomal entrapment and degradation.<sup>21</sup> Secondly, CNTs’ surface can be functionalized with different bioactive species for both targeting and imaging purposes.<sup>22</sup> Surface modification through suitable functional groups can directly improve their aqueous suspendability and reduce their intrinsic cytotoxicity.<sup>23,24</sup> As a matter of fact, CNTs have already been demonstrated in numerous studies as useful nanocarriers for different classes of drugs,<sup>25,26</sup> including bioactive peptides.

In one study, a model penta-peptide and an antigenic epitope from the foot-and-mouth disease virus (FMDV) were covalently conjugated on single-walled carbon nanotubes (SWCNTs).<sup>27</sup> The FMDV peptide-SWCNT conjugate was shown to display an intact peptide’s structure and could be recognized by monoclonal and polyclonal antibodies. Other FMDV peptides have also been coupled to mono- or bis-maleimido-derivatized SWCNTs using selective chemical ligation<sup>28</sup> and the epitopes were shown to be appropriately presented for recognition by antibodies. Notably, strong anti-peptide antibody responses were elicited when these peptide-SWCNT conjugates were administered to mice. In a more recent study, SWCNTs were employed as antigen carriers for poorly immunogenic Wilm’s tumor protein (WT1) peptide 427

against hematopoietic malignancies.<sup>29</sup> WT1 peptide-SWCNT constructs were rapidly internalized *in vitro* into professional antigen presenting cells (APCs, mainly dendritic cells and macrophages) within minutes. Immunization of BALB/c mice with the peptide-SWCNT constructs mixed with immunological adjuvant (TiterMax) induced specific IgG responses against the peptide, while the peptide alone or the peptide mixed with the adjuvant did not induce comparable response. Notably, antibody responses to empty SWCNTs carriers were not detectable *in vivo*.

To advance bioactive peptides for therapeutic application, it is necessary to develop alternative delivery system to address issues pertaining to permeation across biological membrane, lysosomal entrapment, and peptidolytic degradation. In accord, CNTs arise as a promising platform as exemplified by their remarkable capacity to effectively deliver antigenic peptides without compromising peptide’s structural integrity and display for target recognition. In this study, we set out to explore the delivery of the cytotoxic but non-cell-permeable peptide HKII(pep), which possesses intracellular targets on mitochondria, using CNTs. We aimed to improve its therapeutic efficacy against cancer cells and we have demonstrated for the first time that CNTs could serve as excellent vehicle for bioactive HKII peptide delivery with enhanced efficacy over commercially available CPP-HKII(pep) fusion peptide.

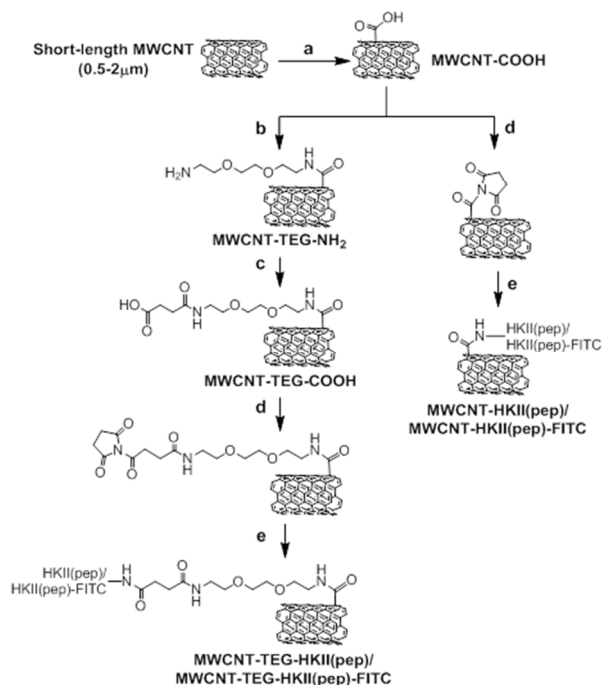
## 2 Results and discussion

### 2.1 Synthesis and characterization of MWCNT/HKII(pep) conjugates

Short-length MWCNTs (0.5-2  $\mu\text{m}$  in length) were chosen as the peptide carrier due to their superior suspendability in aqueous solution and lower intrinsic cytotoxicity.<sup>30,31</sup> Oxidation treatment for 10 h was necessary to eliminate contaminants, further reduce the length to facilitate individualization of the CNTs and generate more carboxylic acid groups for peptide functionalization.<sup>32</sup> Figs. S1a & b demonstrate significant reduction in length after oxidation (100-500 nm), and confirmed that the structural integrity of the tubes was preserved. For loading of HKII(pep) on MWCNTs spaced with a linker, 2,2’-(ethylenedioxy)bis(ethylamine) ( $\text{NH}_2\text{-TEG-NH}_2$ ) was conjugated onto MWCNT-COOH *via* HATU-mediated amide coupling reaction. The amount of loaded linker was estimated by Kaiser test, which measures concentration of primary amine present on the linker. It was found that 446.9  $\mu\text{mol}$  of  $-\text{NH}_2$  groups was present on TEG-functionalized MWCNTs per gram of sample. As HKII(pep) was conjugated *via* its N-terminal  $-\text{NH}_2$  group, conversion of MWCNT-TEG into MWCNT-TEG-COOH was necessary (Scheme 1). Indeed, this reaction was proven to be successful, as denoted by the decrease in Kaiser test value to 163.7  $\mu\text{mol/g}$  for MWCNT-TEG-COOH (ca. 40%). Taking the difference of the Kaiser test values before and after reacting with succinic anhydride, the

amount of  $-COOH$  converted was estimated to be  $283.3 \mu\text{mol/g}$  for MWCNT-TEG-COOH, corresponding to approximately 60% of  $-COOH$  conversion.

HKII(pep) was loaded on MWCNT-COOH directly or MWCNT-TEG-COOH *via* amide coupling through its N-



**Scheme 1.** Synthetic scheme for the fabrication of the CNTs drug delivery system. a) 98% sulphuric acid: 65% nitric acid = 3:1 v/v, 10 h; b) (Ethylenedioxy)bis-ethylamine, HATU, DIPEA, DMF, stir at  $40^\circ\text{C}$ , 12 h; c) succinic anhydride, stir at  $40^\circ\text{C}$ , 12 h; d) NHS, EDC, DMAP, DIPEA, DMF, stir at  $40^\circ\text{C}$ , 2 h; e) HKII(pep)/HKII(pep)-FITC peptide, stir at  $40^\circ\text{C}$ , 72 h.

terminal  $-NH_2$ , giving rise to MWCNT-HKII(pep) and MWCNT-TEG-HKII(pep), respectively. After HKII(pep) conjugation, the peptide loading on MWCNTs was determined indirectly by measuring the residual unconjugated peptide amount before and after reaction using HPLC. The detection wavelengths were set at 230 nm and 280 nm, based on UV absorption of peptide bond and phenylalanine residues (Fig. S2). MWCNT-HKII(pep) and MWCNT-TEG-HKII(pep) were determined to be functionalized with ca.  $208 \mu\text{mol/g}$  HKII peptide corresponding to ca. 37% w/w MWCNTs.

## 2.2 Cellular uptake of HKII(pep)-FITC functionalized MWCNTs

Confocal fluorescence microscopy was employed to investigate cellular uptake and determine the intracellular distribution of HKII(pep) conjugated MWCNTs. To visualize the location of the MWCNT conjugates, the HKII(pep) used was labelled with FITC *via* an additional lysine residue at the C-terminus [HKII(pep)-FITC]. HKII(pep)-FITC was covalently conjugated on MWCNT-COOH and MWCNT-TEG-COOH in a similar fashion and added to MCF-7 cells for 6 h. The FITC labelled MWCNTs were tracked at 519 nm. The nucleus and the

mitochondria were co-stained using Hoechst 33342 and MitoTracker® dyes, respectively.

Cells treated with HKII(pep)-FITC alone did not show obvious green fluorescence signal in their intracellular space. On the other hand, MCF-7 cells incubated with MWCNT-HKII(pep)-FITC or MWCNT-TEG-HKII(pep)-FITC displayed evident intensification of green fluorescence in intracellular space, indicating enhanced cellular uptake compared to HKII(pep)-FITC without carrier (Figs. 1 b & c). Notably, the presence of linker between MWCNTs and HKII(pep)-FITC did not significantly alter cellular uptake and intracellular distribution of the whole conjugate. Importantly, the images revealed that both MWCNT constructs evaded from endolysosome into cytoplasm, unlike the free HKII(pep)-FITC. Nevertheless, it would be supplementary to include lysosomal staining to ascertain this inference.

When we compared the distribution of green fluorescence (FITC-labelled MWCNTs) and red fluorescence (mitochondria dye) in MWCNT-HKII(pep)-FITC and MWCNT-TEG-HKII(pep)-FITC treated MCF-7 cells (Figs. 1 b & c), we observed that both fluorescent nanoconjugates seemingly colocalized with mitochondria (indicated by white arrows). This indicates the possibility that HKII(pep), after conjugation onto MWCNTs, was able to display its structure properly for target recognition on the OMM. Our findings echo with the report of the successful mitochondrial targeting of MWCNTs using a 25 amino acid long mitochondrial targeting signal peptide derived from the N-terminal region of human cytochrome *c* oxidase.<sup>33</sup> Although the major focus in that study was to target MWCNTs to mitochondria by functionalization with the signal peptide, we reason that the loaded peptide must have been displayed on MWCNTs properly for recognition by mitochondrial import receptors TOM70 and TOM20 on the OMM.<sup>34</sup> Hence, in our case, correct display of HKII(pep) on MWCNTs could have rendered an intracellular distribution pattern reflecting mitochondrial localization, similar as the reported HKII(pep) delivered by arginine based CPP.<sup>9</sup>

These findings validated our hypothesis that functionalized MWCNTs could facilitate the cellular entry of HKII(pep). Importantly, MWCNT-HKII(pep)-FITC and MWCNT-TEG-HKII(pep)-FITC were found to be in the vicinity of mitochondria, which prompted us to investigate whether such phenomenon would be harnessed to improve efficacy *in vitro*.

## 2.3 Cytotoxicity assay of HKII(pep)-functionalized MWCNTs

In light of the promising findings from cellular uptake study, we proceeded to evaluate the efficiency of HKII(pep) conjugated MWCNTs in eliciting toxicity in cancer cells. A two-way ANOVA was conducted to examine the effect of varying concentrations of different treatments, namely HKII(pep), commercially available cell permeable HKII(pep) [CPP-HKII(pep)], MWCNT-HKII(pep), MWCNT-TEG-HKII(pep), on cell survival. In MCF-7 cells, there was a statistically significant interaction between the effects of treatments and concentrations on cell survival,  $F(6, 24) = 7.60$ ,

$p = 0.0001$ . Similarly, a statistical significant interaction was obtained in HCT116 cells between the effects of treatments and concentrations on cell survival,  $F(6, 24) = 13.08$ ,  $p < 0.0001$ .

We found that HKII(pep) alone was not cytotoxic in cancerous MCF-7 and HCT116 cells, with at least 90% of cells being viable even after treatment with 50  $\mu\text{M}$  of HKII(pep) for 48 h (Fig. 2). This was consistent with our findings obtained from confocal microscopy (Fig. 1a), which suggested that HKII(pep) alone were incapable of permeating cellular membrane and travel to their subcellular site of action. In

contrast, simple main effects analysis showed that CPP-HKII(pep) was statistically more cytotoxic in MCF-7 cells across all concentration ranges (Fig. 2). Meanwhile in HCT116 cells, CPP-HKII(pep) was significantly more cytotoxic than HKII(pep) at 50  $\mu\text{M}$ . This emphasizes the need of permeability enhancer, in this case the internalization sequence of the Antennapedia homeoprotein, for realizing the cytotoxic activity of HKII peptide that is, otherwise, “inert” to cells due to poor cellular internalization.

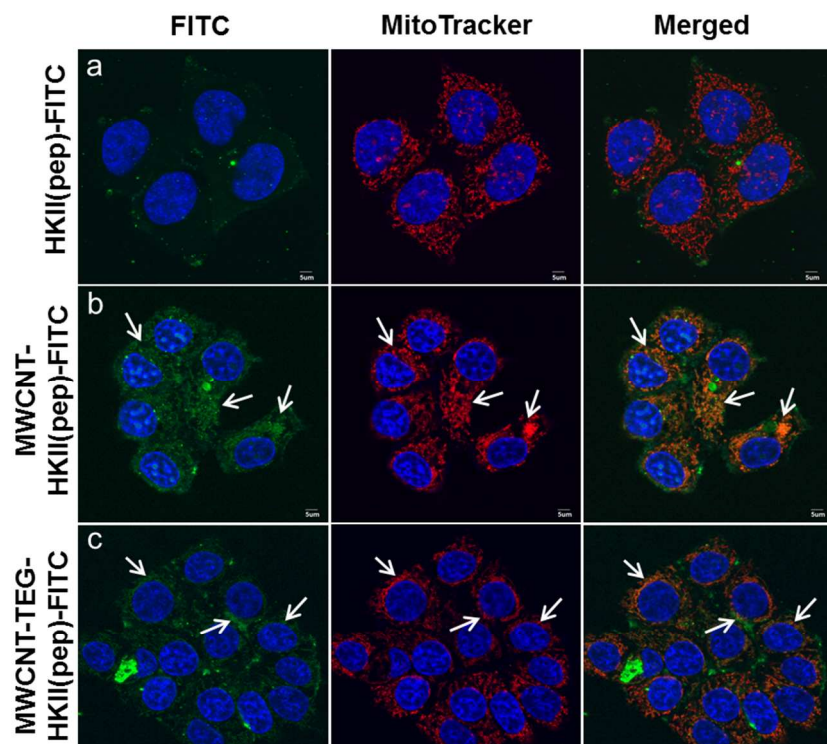


**Fig. 1.** Confocal images of MCF-7 cells incubated with 25  $\mu\text{M}$  HKII(pep)-FITC, 50  $\mu\text{g}/\text{mL}$  MWCNT-HKII(pep)-FITC, or 50  $\mu\text{g}/\text{mL}$  MWCNT-TEG-HKII(pep)-FITC. Images showing green fluorescence indicate uptake of FITC labelled HKII(pep) or the corresponding nanoconjugates. Nuclei and mitochondria were stained with Hoechst 33342 (blue) and Mitotracker<sup>®</sup> Deep Red FM (red). Superimposed images are also shown (merge). Confocal images showed minute cellular uptake of HKII(pep)-FITC (first panel, a), while HKII(pep)-FITC carried by MWCNTs displayed enhanced cellular uptake (second (b) and third panel (c)). Similarity in location of green [HKII(pep)-FITC on MWCNTs] and red fluorescence (mitochondria) are highlighted by white arrows.

Growth inhibitory activity of MWCNT-peptide conjugates in HCT116 and MCF-7 cells were evaluated *via* WST-1 cytotoxicity assay.<sup>35</sup> Treatment with MWCNT-HKII(pep) and MWCNT-TEG-HKII(pep) resulted in a dose-dependent decrease in cell viability (Figs. 2a & b). Comparing CPP-HKII(pep) with HKII(pep) carried by MWCNTs, HKII(pep)'s cancer cell killing efficacy was significantly enhanced using the MWCNTs carrier according to simple main effects analysis. This is evidently pronounced in HCT116 cells in which both MWCNTs constructs were significantly more cytotoxic than CPP-HKII(pep) at all concentrations (Fig. 2b). Notably, at peptide concentration of 25  $\mu\text{M}$ , more than 2-fold reduction in cell viability compared to CPP-HKII(pep) was observed in HCT116 cells when short-length MWCNTs were employed as carrier. On the other hand, MCF-7 cells only retained 10% of

cell viability after being treated with 50  $\mu\text{M}$  MWCNT-HKII(pep) or MWCNT-TEG-HKII(pep). This is significantly lower than ca. 40 % survival in CPP-HKII(pep) treated cells. In short, we found that the HKII(pep) conjugated MWCNTs at 25  $\mu\text{M}$  of peptide concentration exhibited a 50% improvement in cytotoxicity compared to HKII(pep) alone (Fig. 2). Additionally, HKII(pep) conjugated MWCNTs also compared favourably against the commercially available cell permeable HKII fusion peptide carried by Antennapedia based CPP. This superiority over peptide-based delivery system could be attributed to the fact that, while CPP might not have precluded CPP-cargo conjugates from being endocytosed and peptidolytically processed in lysosomes,<sup>36</sup> our MWCNTs constructs explicitly evaded from endosomal entrapment and seemingly distributed to mitochondria (Fig. 1). Nevertheless, it

would be intriguing to evaluate stability of HKII(pep) conjugated MWCNTs in the presence of peptidase to confirm the role of MWCNTs as protective peptide carrier.

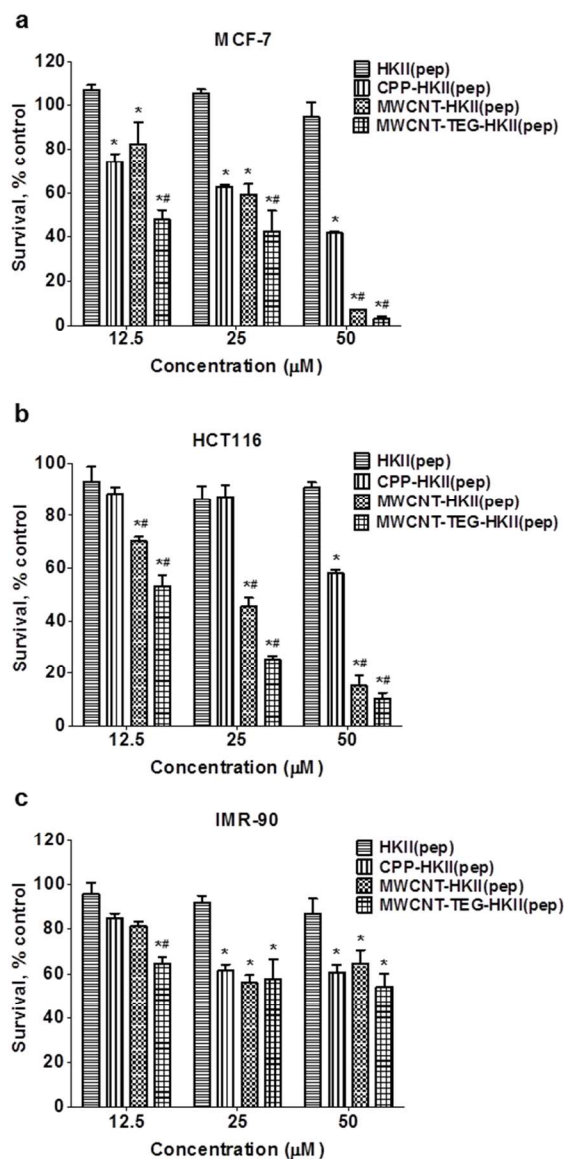


**Fig. 2.** Investigation of cell viability *via* MTT assay or WST-1 assay. HCT116, MCF-7, and IMR-90 cells were treated with 3 concentrations (12.5, 25, 50 μM) of HKII(pep); CPP-HKII(pep); MWCNT-HKII(pep); MWCNT-TEG-HKII(pep) for 48 h. MTT assay was used to assess viability of cells treated with HKII(pep) and CPP-HKII(pep) while WST-1 assay was used to assess viability of cells treated with MWCNT-HKII(pep) and MWCNT-TEG-HKII(pep). MTT/WST-1 readings from the control lane (i.e. cells without any treatment) were used as reference values for 100% survival. \* indicates  $P < 0.05$  compared to HKII(pep) based on two-way ANOVA and Bonferroni post analysis. # indicates  $P < 0.05$  compared to CPP-HKII(pep) based on two-way ANOVA and Bonferroni post analysis. For all panels, data represent three observations for each experiment and are expressed as mean  $\pm$  S.E. ( $n=3$ )

In MCF-7 cells, significant difference in cell survival was observed between MWCNT-HKII(pep) and MWCNT-TEG-HKII(pep) treatment only at 12.5 μM. Meanwhile in HCT116 cells, MWCNT-TEG-HKII(pep) was more cytotoxic than MWCNT-

HKII(pep) at 12.5 μM and 25 μM but not at 50 μM. Collectively we infer that the presence of linkers between MWCNTs and HKII(pep) does not impact the peptide's bioactivity. Moreover based on the observations from cellular uptake studies, it is apparent that the presence of a linker between MWCNTs and HKII(pep) does not affect intracellular distribution of the resulting constructs. We reason that, as HKII(pep) contains fifteen amino acids, the presence of a mere 6-carbon TEG linker might be insignificant in decreasing steric hindrance. Nevertheless, it would be interesting to functionalize MWCNTs with cleavable linkers, i.e. disulfide-based or enzyme-sensitive linkers, for HKII(pep) delivery and compare the efficacy. Indeed, it was reported that cytotoxicity of covalently conjugated active moiety strongly depends on the type of cleavable linker used on MWCNTs.<sup>37</sup>

All the constructs were also tested in human fetal lung fibroblast IMR-90. A two-way ANOVA was also conducted to examine the effect of varying concentration of different treatments on cell survival. The interaction between the effects of treatments and concentrations on cell survival was found to be statistically insignificant,  $F(6, 23) = 1.52, p = 0.2165$ . To our surprise, HKII(pep) coupled with delivery carrier, be it either Antennapedia-based internalization sequence or our MWCNT-based nanocarrier, exerted detectable toxic effects on this cell line, with ca. 40% reduction in cell viability at the highest tested concentration of 50 μM (Fig. 2c). This could be due to the considerable expression of HKII(pep) in this cell line, leading to the slight toxicity observed ensuing entry of HKII(pep).<sup>38</sup> Nevertheless, the ability of HKII(pep) in deterring cancerous MCF-7 and HCT116 cell growth was still significantly more profound compared to its effect in IMR-90 cells. However, studies in other non-cancerous cell lines are essential to further confirm the selectivity towards cancer cells. If deemed necessary, active targeting by folic acid or RGD peptide could be devised on our MWCNT constructs to attain more preferential killing of cancer cells.<sup>39</sup>

To ascertain that the cytotoxicity observed with HKII(pep) conjugated MWCNTs construct was due to the activity of HKII(pep) rather than the intrinsic toxicity of MWCNTs, we performed WST-1 assay on cells exposed to the empty carrier (Fig. S3). It was back-calculated from peptide loading that there was ca. 240 μg/mL of MWCNTs at a corresponding highest HKII(pep) concentration of 50 μM for both nano-constructs (with or without linker). We found that at highest MWCNTs concentration of 250 μg/mL, MWCNT-COOH did not elicit significant toxicity in HCT116, MCF-7, and IMR-90 with at least 80% of cells remained viable (Fig. S3a). On the other hand, treatment of 250 μg/mL of MWCNT-TEG-COOH in all three cell lines resulted in ca. 40% drop in cell viability, signifying that toxicity of MWCNT-TEG-COOH was higher than MWCNT-COOH. Nevertheless, compared to cells treated with HKII(pep) loaded MWCNT-TEG-HKII(pep) that rendered less than 20% in viability, we conclude that the majority of the effect observed stemmed from the bioactivity of HKII(pep) rather than MWCNT-TEG-COOH's intrinsic cytotoxicity.

Taken together with the observations from confocal microscopy (Figs. 1b & c), these results implied that MWCNTs as delivery system potentiated the efficacy of HKII(pep) primarily by increasing their availability inside the cells.

#### 2.4 MWCNT-HKII(pep) and MWCNT-TEG-HKII(pep) depleted cellular energy and induced apoptosis

In malignant cancers with highly glycolytic phenotype, after rapid entry of glucose into cancer cells *via* the glucose transporter, HKII becomes the main facilitator for active glycolysis.<sup>4</sup> It binds to the OMM *via* VDAC, which, together with the ANT at IMM, transports ATP newly synthesized by ATP synthase (housed at the IMM) to HKII.<sup>6</sup> This positional

advantage enables the enzyme to produce glucose-6-phosphate conveniently and leads to elevated glycolytic activity for production of building blocks and ATP to support tumour growth. In light of this, intracellular ATP level was measured to examine if energy production in HCT116 was affected after exposure to HKII(pep) coupled on MWCNTs. Following addition of 25  $\mu$ M of MWCNT-HKII(pep) or MWCNT-TEG-HKII(pep), intracellular ATP level declined steadily after 2 h and further plunged with prolonged treatment (Fig. 3a). After 8 h of incubation with HKII(pep) conjugated MWCNTs, cellular ATP level displayed a pronounced decrease to around 50%. On the contrary, incubation with either 25  $\mu$ M HKII(pep), MWCNT-COOH, or MWCNT-TEG-COOH was unable to

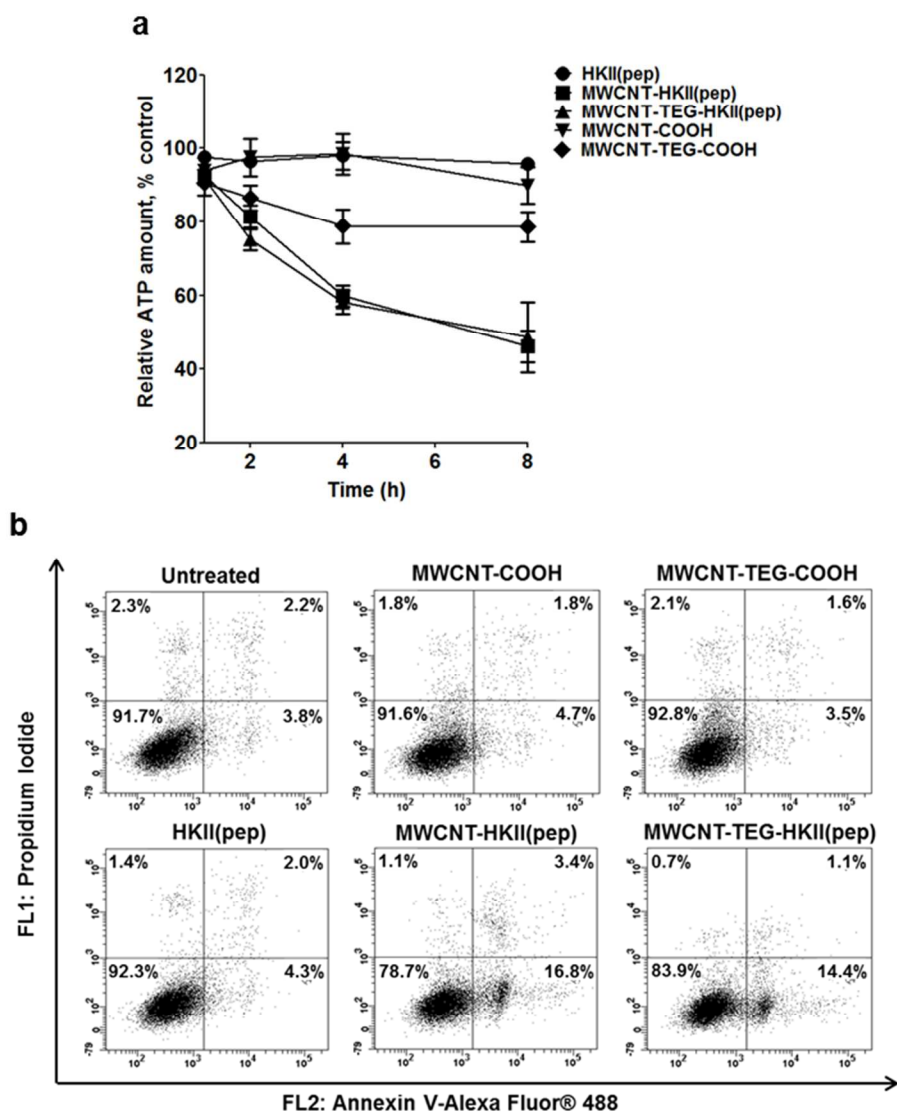


**Fig. 3.** a) Quantitation of ATP level in HCT116 cells after different treatment. HCT116 cells were treated with 25  $\mu$ M HKII(pep); 25  $\mu$ M MWCNT-HKII(pep); 25  $\mu$ M MWCNT-TEG-HKII(pep); 125  $\mu$ g/mL MWCNT-COOH; 125  $\mu$ g/mL MWCNT-TEG-COOH for the indicated times. The intracellular ATP level was measured using CellTiter-Glo Luminescent Cell Viability Assay kit. The points represent the mean  $\pm$  S.E. (n=3); b) Investigation of mechanism of cell death after 2 h incubation of HKII(pep) (25  $\mu$ M), MWCNT-HKII(pep) (25  $\mu$ M), MWCNT-TEG-HKII(pep) (25  $\mu$ M), MWCNT-COOH (125  $\mu$ g/mL), or MWCNT-TEG-COOH (125  $\mu$ g/mL) in HCT116 cells followed by annexin V/PI staining before analysing with flow cytometry. Left bottom quadrant represents live cells (annexin V/PI negative). Right bottom quadrant represents early apoptotic cells (annexin V positive/PI negative). Right upper quadrant represents necrotic/late apoptotic cells (annexin V/PI positive).

impact ATP metabolism in cells, demonstrated by the slight reduction in ATP content.

On the other hand, the ability of HKII(pep) in inducing apoptosis was examined after its conjugation on MWCNTs. HCT116 cells were treated with 25  $\mu$ M MWCNT-HKII(pep) or MWCNT-TEG-HKII(pep) or respective controls for 2 h. The ability of our constructs in eliciting apoptosis was validated by annexin V/PI staining. Apoptosis is distinguished from necrosis by characteristic morphological and biochemical changes, including compaction and fragmentation of the nuclear chromatin, shrinkage of the cytoplasm, and loss of membrane asymmetry.<sup>40</sup> In apoptotic cells, phosphatidylserine is translocated from the cytoplasmic surface to the outer leaflet of plasma membrane and the exposed phosphatidylserine is recognized by the human anticoagulant annexin V with high affinity.<sup>41</sup> Neither free HKII(pep) without carrier, nor plain carrier (MWCNT-COOH or MWCNT-TEG-COOH) induced apparent apoptotic events in HCT116 cells, as evidenced by the comparable extent of cell death with untreated control (Fig. 3b, first row). Conversely, 16.8% and 14.4% of MWCNT-HKII(pep) and MWCNT-TEG-HKII(pep) treated cells, respectively, manifested signs of early apoptosis indicated by a positive staining with Alexa Fluo® 488 conjugated Annexin V (Fig. 3b, bottom row). Concordant with previous findings in this report, both constructs of HKII(pep) carried by MWCNTs (with or without linker) had no discernible difference in terms of peptide efficiency.

### 2.5 HKII(pep) conjugated on MWCNTs indeed triggered HKII release from mitochondria

To validate if all abovementioned effects of MWCNT-HKII(pep) or MWCNT-TEG-HKII(pep) on HCT116 cells truly arose from the activity of HKII(pep), which is the ability to compete with HKII for binding on mitochondria, we carried out immunoblotting of the endogenous protein in mitochondria-enriched fraction. Indeed, compared to untreated control, HCT116 cells treated with 25  $\mu$ M of MWCNT-HKII(pep) or MWCNT-TEG-HKII(pep) exhibited diminished level of HKII by ca. 40-50% in the mitochondria-enriched fraction. This implies that HKII(pep) on MWCNTs were capable of triggering HKII detachment from mitochondria (Fig. 4, lanes 3 & 4, respectively). In contrast, addition of bare HKII(pep) and empty MWCNT carriers did not result in significant loss of HKII from the mitochondria enriched-fraction (Fig. 4, lanes 2, 5 & 6).

This direct proof highlights the advantage of delivering HKII peptide using MWCNTs without compromising its activity. Together with the observations in intracellular uptake and seemingly mitochondrial distribution, we infer that conjugation of HKII(pep) on MWCNTs did not jeopardize the peptide display for target recognition. Moreover, we have demonstrated for the first time that bioactive HKII peptide could be carried intracellularly by nanocarrier MWCNTs with higher cytotoxic effect on cancer cells compared to conventional CPP delivery system. Essentially, the conjugated peptide was able to compete and displace endogenous HKII

from its association with mitochondria. Our findings indicate an optimistic potential of developing MWCNTs as versatile nanocarrier for bioactive peptides.

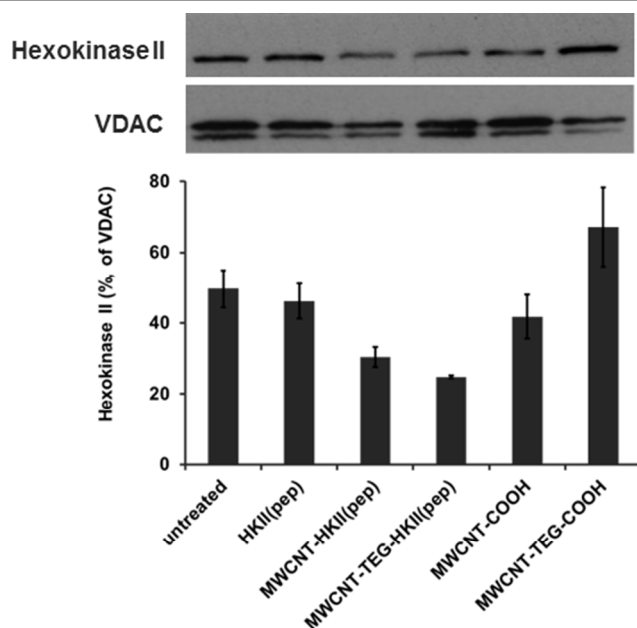


**Fig. 4.** Mitochondria extraction and immunoblotting of hexokinase II. HCT116 cells were treated with HKII(pep) (25  $\mu$ M); MWCNT-HKII(pep) (25  $\mu$ M); MWCNT-TEG-HKII(pep) (25  $\mu$ M); MWCNT-COOH (125  $\mu$ g/mL); MWCNT-TEG-COOH (125  $\mu$ g/mL) for 4 h. Thereafter, the cells were harvested and crude extraction was performed to obtain mitochondria-enriched fraction. Western blot of HKII was performed in the mitochondria-enriched fraction and immunoblot of VDAC was served as loading control. Densitometry of each lane was quantitated using ImageJ (NIH, USA).

## 3 Experimental

### 3.1 Materials

Fifteen amino acid N-terminal peptide sequence of HKII MIASHLLAYFFTELN [HKII(pep)] and its fluorescent derivative (modified with a fluorescein moiety at the additional lysine residue) with sequence MIASHLLAYFFTELNK-FITC [HKII(pep)-FITC] were purchased from Biomatik Corporation (De, USA). Commercially available cell-permeable peptide analogue of HKII (CPP-HKII) was procured from EMD Millipore (Darmstadt, Germany). Short-length MWCNTs were purchased from Nanostructured & Amorphous Materials Inc. (TX, USA). (Ethylenedioxy)bis-ethylamine (TEG), *N,N*-Diisopropylethylamine (DIPEA), *N*-hydroxysuccinimide (NHS), 3-(4,5-Dimethylthiazol-2-yl)-2,5-diphenyltetrazolium bromide (MTT), Sucrose, (4-(2-hydroxyethyl)-1-piperazineethanesulfonic acid) (HEPES), potassium chloride (KCl), magnesium chloride (MgCl<sub>2</sub>), ethylenediaminetetraacetic acid (EDTA), and ethylene glycol tetraacetic acid (EGTA) were procured from Sigma Aldrich (MO, USA). *O*-(7-azabenzotriazol-1-yl)-*N,N,N',N'*-tetramethyluronium hexafluorophosphate (HATU), 4-

(dimethylamino)pyridine (DMAP) and 2,2'-Diaminodiethyl disulfide dihydrochloride (cystamine) were purchased from Alfa Aesar (Lancaster, UK). 1-Ethyl-3-(3-dimethylaminopropyl) carbodiimide hydrochloride (EDC) was purchased from GL BioChem (Shanghai, China). Potassium cyanide (KCN) was kindly provided by teaching lab of pharmacy department, National University of Singapore. Dulbecco's modified Eagle's medium (DMEM), fetal bovine serum (FBS), and protease inhibitor cocktail were procured from Thermo Scientific (MA, USA). RPMI-1640, McCoy's 5A medium, and TrypLE™ Express Enzyme were purchased from Life Technologies (CA, USA). 4-[3-(4-Iodophenyl)-2-(4-(nitrophenyl)-2H-5-tetrazolio)-1,3-benzene disulfonate (WST-1) was purchased from Roche Applied Science (IN, USA). CellTiter-Glo Luminescent Cell Viability Assay kit was purchased from Promega Corp. (WI, USA). Dimethyl formamide (DMF) and dimethyl sulfoxide (DMSO) were obtained from Merck Millipore (Darmstadt, Germany). Bradford reagent was procured from Bio-Rad Laboratories Inc. (CA, USA). Antibodies to VDAC-1 (20B12) and HKII (C-14) were purchased from Santa Cruz Biotechnology Inc. (TX, USA).

### 3.2 Functionalization of CNTs for peptide delivery

The synthetic scheme starting from the functionalization of the CNT carrier to the final attachment of HKII(pep) is summarized in Scheme 1. Pristine short-length MWCNTs (20 mg) were oxidized for 10 h by sonication in 98% sulphuric acid: 65% nitric acid (3:1 v/v, 4 mL) to create the carboxylic acid groups needed for subsequent functionalization. The oxidized MWCNTs were then purified and recovered, yielding MWCNT-COOH (19 mg).<sup>42</sup>

In order to add amine-terminated 2,2'-(ethylenedioxy)bis(ethylamine) (TEG) groups, oxidized MWCNT-COOH (15 mg, 45  $\mu$ mol of COOH) was reacted with TEG, yielding MWCNT-TEG-NH<sub>2</sub>, according to previous report.<sup>42</sup>

The conversion of free terminal amino group present on the linker TEG into COOH group allowed the HKII(pep) to be linked to the CNTs *via* its N-terminal amine. 8 mg of MWCNT-TEG-NH<sub>2</sub> were reacted with 30 equivalents of succinic anhydride and 2 equivalents of DIPEA in 1 mL of dry DMF. The reaction mixture was then stirred at 40°C for 12 h. The eventual MWCNT-TEG-COOH was then harvested *via* filtering through a 0.2  $\mu$ m PTFE membrane, and rinsed thoroughly with DMF, followed by methanol and DI water. The MWCNTs were subsequently recovered from the membrane with additional DI water and lyophilized, giving 7.5 mg of MWCNT-TEG-COOH. TEG loading on MWCNT-TEG-NH<sub>2</sub> and the conversion into -COOH were estimated by quantitative Kaiser test.<sup>42</sup> Briefly, the primary amine on MWCNT-TEG-NH<sub>2</sub> would generate relatively higher Kaiser test readout. As for MWCNT-TEG-COOH, the decrease in Kaiser test readout represent the extent of conversion into carboxylic acid.

### 3.3 Conjugation of HKII(pep)/HKII(pep)-FITC on MWCNTs

MWCNT-COOH and MWCNT-TEG-COOH were further functionalized with HKII(pep), yielding MWCNT-HKII(pep) and MWCNT-TEG-HKII(pep), respectively. Briefly, 5 equivalent of EDC-HCl, 5 equivalents of NHS and 2  $\mu$ L of DIPEA were added into 0.5 mL of dry DMF in the presence of a catalytic amount of DMAP before addition of the CNTs. The reaction mixture was then stirred at 60°C for 2 h. The resulting carboxylic activated MWCNTs were then filtered through a 0.2  $\mu$ m PTFE membrane and washed 4 times with 100  $\mu$ L of dry DMF. The MWCNTs were recovered from the membrane with 500  $\mu$ L of dry DMF. Two equivalents of HKII(pep) were reconstituted in 500  $\mu$ L of dry DMF with 4% DMSO. 10  $\mu$ L of the reconstituted peptide solution was kept for HPLC analysis and the remaining solution was then added to the carboxylic activated MWCNTs in DMF and allowed to react at 40°C for 72 h. The reaction mixture was then filtered through a 0.2  $\mu$ m PTFE membrane, and rinsed thoroughly with DMF, followed by methanol and DI water. The filtrate and DMF washes were collected for subsequent HPLC analysis for estimation of peptide loading. The MWCNTs were recovered from the membrane with additional DI water and lyophilized.

HKII(pep)-FITC functionalization on MWCNT-COOH or MWCNT-TEG-COOH for confocal microscopy was performed similarly to the abovementioned HKII(pep) conjugation.

### 3.4 Estimation of peptide loading *via* HPLC

As MWCNTs could not be injected directly into a reversed phase HPLC C-18 column, estimation of peptide loading was carried out indirectly by subtracting the amount of unreacted peptide after reaction from the total peptide before reaction. A calibration curve was constructed by injecting a series of calibration (standard) solutions of known HKII(pep) concentration and a standard graph with response (area under curve) versus concentration was obtained. HKII(pep) solutions of differing concentrations were prepared (3.5 mg/mL, 1.75 mg/mL, 0.88 mg/mL, 0.44 mg/mL, and 0.22 mg/mL). All the samples were analyzed using Agilent 1200 Series HPLC System fitted with Waters XTerra RP18 Column, 5  $\mu$ m, 4.6 x 150 mm column. The analysis was conducted at a gradient of 35% acetonitrile (ACN)/65% H<sub>2</sub>O to 65% ACN/ 35% H<sub>2</sub>O in 10 min with flow rate of 0.8 mL/min.

### 3.5 Cell culture

Human breast cancer cells MCF-7 and human colon carcinoma HCT116 were selected as cancer prototypes to evaluate suitability of CNTs as drug delivery system for bioactive HKII(pep) due to their reported usage in HKII-related study.<sup>15,43</sup> Human fetal lung fibroblasts IMR-90 were employed as non-cancerous control. MCF-7, HCT116, and IMR-90 were purchased from ATCC (VA, USA) and maintained in RPMI 1640, McCoy's 5A, and DMEM, respectively. All media were supplemented with 10% FBS and the cells were incubated at

37°C in humidified air containing 5% CO<sub>2</sub>. All cells were sub-cultured every 3 to 4 days with TrypLE™ Express Enzyme.

### 3.6 Uptake and intra-cellular distribution of HKII (pep) functionalized MWCNTs

Confocal microscopy was conducted to investigate cellular uptake and intra-cellular distribution of HKII(pep)-FITC conjugated on MWCNT-COOH and MWCNT-TEG-COOH, respectively. Briefly, MCF-7 cells were seeded in a 29 mm glass bottom dish (In Vitro Scientific, USA) at a density of  $5 \times 10^4$  cells/mL for 24 h, followed by incubation with 25  $\mu$ M of HKII(pep)-FITC peptide, 50  $\mu$ g/mL of MWCNT-HKII(pep)-FITC or MWCNT-TEG-HKII(pep)-FITC for 6 h. Thereafter, the cells were incubated with Hoechst 33342 (5  $\mu$ g/mL) for 10 min as a nuclear counter-stain, followed by MitoTracker® Deep Red FM (25 nM) for 5 min to stain mitochondria before being viewed under a confocal microscope (Confocal Laser Scanning Biological Microscope FV10i, Olympus). HKII(pep)-FITC functionalized MWCNTs, MitoTracker® Deep Red FM, and Hoechst 33342 were excited at 495 nm, 635 nm, and 352 nm, respectively. Fluorescence emission was recorded at 519 nm, 690 nm, and 455 nm for HKII(pep)-FITC functionalized MWCNTs, MitoTracker® Deep Red FM, and Hoechst 33342, respectively.

### 3.7 Cytotoxicity Assay

MTT assay was used for experiments involving HKII(pep) and its cell-permeable analogue CPP-HKII(pep), while WST-1 assay was employed for experiments involving CNTs, as CNTs could bind to the insoluble MTT formazan crystals and artificially lower the measured absorbance values.<sup>35</sup> WST-1 produces a water-soluble formazan product and is hence able to resolve this inaccuracy.

To perform the cytotoxicity assay, cells were first seeded into 96-well tissue culture plates (Costar, Corning NY) at a density of  $1 \times 10^4$  cells/well for IMR-90 and HCT116, and 8,000 cell/well for MCF-7. After 24 h, the medium was removed and the cells were exposed to varying concentrations of test compounds. HKII(pep) loading was used to calculate the amount of MWCNTs needed to prepare corresponding test concentration of peptide. After another incubation of 48 h, the medium was aspirated, replaced with 100  $\mu$ L of either MTT (0.5 mg/mL in PBS) or WST-1 (1:15 dilution from ready-to-use stock in PBS), and incubated for 4 h or 30 min, respectively. For MTT assay, the MTT solution was removed and DMSO was added to dissolve the insoluble purple formazan crystals. For WST-1 assay, 80  $\mu$ L of the WST-1 solution without cells or MWCNTs was aspirated for subsequent absorbance reading. The absorbance of the assayed solution was measured at 595nm for MTT and 440nm for WST-1 using a microplate reader (BioTek™ Synergy™ H1 Hybrid Multi-Mode Microplate Reader). Experiments were performed in three repeats for at least three replicates. The data were analyzed using GraphPad Prism (Version 6.0, GraphPad Software).

### 3.8 Apoptosis/necrosis staining and flow cytometry

For apoptosis/necrosis staining, HCT116 cells were seeded in 12-well culture plate (SPL Life Sciences Co. Ltd., Korea) at  $1 \times 10^5$  cells/well and allowed to grow for 72 h. The cells were then given different treatments for 2 h. All cells were harvested and stained at density of  $1 \times 10^6$  cells/mL with 2  $\mu$ L of Alexa Fluor® 488 conjugated Annexin V and 0.1  $\mu$ g of propidium iodide (PI) for 15 min at room temperature. All cell samples were immediately analyzed by flow cytometry using BD LSRFortessa™ Flow Cytometry Analyser (BD Biosciences, USA). Alexa Fluor® 488 conjugated Annexin V was excited using 488 nm laser and PI was excited using 561 nm laser. Fluorescence emissions were recorded at 530 nm and 575 nm for Alexa Fluor® 488 conjugated Annexin V and PI, respectively.

### 3.9 ATP quantitation

HCT116 cells were seeded at  $2 \times 10^4$  cells/well in 96-well culture plate and allowed to grow for 48 h. Different treatments were given for 1 h, 2 h, 4 h, and 8 h. ATP level in cells was then quantitated using CellTiter-Glo Luminescent Cell Viability Assay kit according to manufacturer's protocol. Luminescence was measured by BioTek™ Synergy™ H1 Hybrid Multi-Mode Microplate Reader from BioTek Instruments Inc. (VT, USA).

### 3.10 Mitochondria extraction and immunoblotting of HKII

Mitochondria isolation was performed as previously described.<sup>44,45</sup> Briefly, a total of  $1 \times 10^7$  cells were resuspended in mitochondria isolation buffer (250 mM Sucrose, 20 mM HEPES-NaOH [pH 7.9], 10 mM KCl, 1.5 mM MgCl<sub>2</sub>, 1 mM EDTA, 1 mM EGTA) supplemented with protease inhibitor cocktail and disrupted by 20 strokes through a 25 gauge needle followed by centrifugation at  $800 \times g$  for 10 min at 4°C. Supernatants were centrifuged twice at  $12,000 \times g$  for 20 min each at 4°C to pellet the heavy membrane fraction enriched with mitochondria for the analysis of HKII. Immunoblotting was carried out as described.<sup>46</sup> Protein concentration of each sample was determined by Bradford assay. An equal amount of proteins for each sample was subjected to fractionation on SDS-PAGE, followed by western blotting analysis for HKII and VDAC-1. Densitometry of each lane was quantitated using ImageJ (NIH, USA).

### 3.11 Statistical analysis

All experiments were performed in triplicate unless otherwise stated. Results of experimental repeats for cytotoxicity assay, intracellular ATP quantification, and western blot densitometry were input into Graphpad Prism 5 (Ca, USA) and corresponding plot with mean and SEM were obtained. For cytotoxicity assay, statistical significance was assessed using two-way ANOVA comparing treatment groups [HKII(pep), CPP-HKII(pep), MWCNT-HKII(pep), MWCNT-TEG-HKII(pep)] and concentrations followed by post-hoc analysis

with Bonferroni test with  $p < 0.05$  considered significant. These statistical analyses were performed using Graphpad Prism 5.

#### 4 Conclusion

Two different conjugates, MWCNT-HKII(pep) and MWCNT-TEG-HKII(pep), were successfully synthesized by amide coupling. Both constructs were internalized intracellularly and displayed considerably higher degree of cellular uptake compared to peptide without carrier. Notably, a tendency of both nano-conjugates to adopt an intracellular dissemination pattern resembling mitochondria distribution was observed. Cytotoxicity assays suggested that conjugation of HKII(pep) on MWCNTs with or without linker did not hinder the peptide from exerting its bioactivity. 2-fold enhancement in peptide cytotoxic action was observed with HKII(pep) conjugated MWCNTs compared to commercially available CPP-HKII(pep). Moreover, MWCNTs delivery system was superior to commercially available CPPs in terms of efficacy enhancement. The MWCNT-peptide conjugates were able to elicit apoptosis and decrease ATP level in cells. Importantly, HKII(pep) covalently conjugated on MWCNTs was shown to compete with endogenous HKII for binding on to mitochondria, emphasizing the immense potential of MWCNTs as effective nanocarriers for peptide delivery.

#### Acknowledgements

This research has been supported by the National University of Singapore, Department of Pharmacy ((AcRF) Tier 1-FRC grant R-148-000-164-112) and by MOE of Singapore (grant MOE2011-T21-1201-P09; R-144-000-306-112). NGS graduate fellowship is thankfully acknowledged by S.L.Y. for financial support of her graduate study. Also, we would like to thank NUHS flow cytometry laboratory, Ms. Wang Xiaoning and Ms. Toh Chin Min for supports in flow cytometry experiments. Last but not least, the estimation of peptide loading by reversed phase HPLC analysis would not have been accomplished without the kind help from Ms. Tang Shi Qing, Dr Pandy Murugappan Ramanujulu, Prof. Christina Chai, Prof. Brian Dymock from Department of Pharmacy.

#### Notes

<sup>a</sup> NUS Graduate School for Integrative Sciences and Engineering, Centre for Life Sciences (CeLS), 28 Medical Drive, Singapore 117456.

<sup>b</sup> Department of Pharmacy, National University of Singapore, 3 Science Drive 2, Singapore 117543. Email: [phaps@nus.edu.sg](mailto:phaps@nus.edu.sg); Fax: +65-67791554; Tel: +65-65161876

<sup>c</sup> Electrical and Computer Engineering, National University of Singapore, Engineering Drive 3, Singapore 117576.

<sup>d</sup> Department of Chemistry, National University of Singapore, 3 Science Drive 2, Singapore 117543. Email: [chmawh@nus.edu.sg](mailto:chmawh@nus.edu.sg); Fax: +65-67791691; Tel: +65-65165131

<sup>e</sup> NanoCore, Engineering Block A, Faculty of Engineering, National University of Singapore, Singapore 117576.

† Electronic Supplementary Information (ESI) available: Additional TEM images, UV-Vis scanning characterisation, WST-1 assay results, and immunoblotting of HKII in total cell lysate. See DOI: 10.1039/b000000x/

#### References

1. J. E. Wilson, *J. Exp. Biol.*, 2003, **206**, 2049-2057.
2. D. Sui and J. E. Wilson, *Arch Biochem Biophys*, 1997, **345**, 111-125.
3. J. G. Pastorino and J. B. Hoek, *J Bioenerg Biomembr*, 2008, **40**, 171-182.
4. S. P. Mathupala, A. Rempel and P. L. Pedersen, *J Biol Chem*, 2001, **276**, 43407-43412.
5. P. L. Pedersen, S. P. Mathupala, A. Rempel, J. F. Geschwind and Y. H. Ko, *Biochim Biophys Acta*, 2002, **1555**, 14-20.
6. S. P. Mathupala, Y. H. Ko and P. L. Pedersen, *Oncogene*, 2006, **25**, 4777-4786.
7. M. G. Vander Heiden, L. C. Cantley and C. B. Thompson, *Science*, 2009, **324**, 1029-1033.
8. J. G. Pastorino, N. Shulga and J. B. Hoek, *J Biol Chem*, 2002, **277**, 7610-7618.
9. N. Majewski, V. Nogueira, P. Bhaskar, P. E. Coy, J. E. Skeen, K. Gottlob, N. S. Chandel, C. B. Thompson, R. B. Robey and N. Hay, *Mol Cell*, 2004, **16**, 819-830.
10. S. Fulda, L. Galluzzi and G. Kroemer, *Nat Rev Drug Discov*, 2010, **9**, 447-464.
11. S. Ganapathy-Kanniappan, M. Vali, R. Kunjithapatham, M. Buijs, L. H. Syed, P. P. Rao, S. Ota, B. K. Kwak, R. Loffroy and J. F. Geschwind, *Curr Pharm Biotechnol*, 2010, **11**, 510-517.
12. E. Flescher, *Cancer Lett*, 2007, **245**, 1-10.
13. D. D. Meira, M. M. Marinho-Carvalho, C. A. Teixeira, V. F. Veiga, A. T. Da Poian, C. Holandino, M. S. de Freitas and M. Sola-Penna, *Mol Genet Metab*, 2005, **84**, 354-362.
14. F. Chiara, D. Castellaro, O. Marin, V. Petronilli, W. S. Brusilow, M. Juhaszova, S. J. Sollott, M. Forte, P. Bernardi and A. Rasola, *PLoS One*, 2008, **3**, e1852. Available from URL: <http://www.ncbi.nlm.nih.gov/pmc/articles/PMC2267038/>.
15. N. Shulga, R. Wilson-Smith and J. G. Pastorino, *Cell Cycle*, 2009, **8**, 3355-3364.
16. C. Palm, M. Jayamanne, M. Kjellander and M. Hallbrink, *Biochim Biophys Acta*, 2007, **1768**, 1769-1776.
17. A. Erazo-Oliveras, N. Muthukrishnan, R. Baker, T. Y. Wang and J. P. Pellois, *Pharmaceuticals (Basel)*, 2012, **5**, 1177-1209.
18. N. R. Soman, S. L. Baldwin, G. Hu, J. N. Marsh, G. M. Lanza, J. E. Heuser, J. M. Arbeit, S. A. Wickline and P. H. Schlesinger, *J Clin Invest*, 2009, **119**, 2830-2842.
19. C. Prego, D. Torres, E. Fernandez-Megia, R. Novoa-Carballal, E. Quiñoá and M. J. Alonso, *J Control Release*, 2006, **111**, 299-308.
20. K. Kostarelos, L. Lacerda, G. Pastorin, W. Wu, S. Wieckowski, J. Luangsivilay, S. Godefroy, D. Pantarotto, J. P. Briand, S. Muller, M. Prato and A. Bianco, *Nat Nanotechnol*, 2007, **2**, 108-113.
21. Q. Mu, D. L. Broughton and B. Yan, *Nano Lett*, 2009, **9**, 4370-4375.
22. S. M. Janib, A. S. Moses and J. A. MacKay, *Adv Drug Deliv Rev*, 2010, **62**, 1052-1063.
23. A. Bianco, K. Kostarelos and M. Prato, *Curr Opin Chem Biol*, 2005, **9**, 674-679.

24. M. Prato, K. Kostarelos and A. Bianco, *Acc Chem Res*, 2008, **41**, 60-68.
25. B. S. Wong, S. L. Yoong, A. Jagusiak, T. Panczyk, H. K. Ho, W. H. Ang and G. Pastorin, *Adv Drug Deliv Rev*, 2013, **65**, 1964-2015.
26. S. Boncel, P. Zajac and K. K. Koziol, *J Control Release*, 2013, **169**, 126-140.
27. D. Pantarotto, C. D. Partidos, R. Graff, J. Hoebeke, J. P. Briand, M. Prato and A. Bianco, *J Am Chem Soc*, 2003, **125**, 6160-6164.
28. D. Pantarotto, C. D. Partidos, J. Hoebeke, F. Brown, E. Kramer, J. P. Briand, S. Muller, M. Prato and A. Bianco, *Chem Biol*, 2003, **10**, 961-966.
29. C. H. Villa, T. Dao, I. Ahearn, N. Fehrenbacher, E. Casey, D. A. Rey, T. Korontsvit, V. Zakhaleva, C. A. Batt, M. R. Philips and D. A. Scheinberg, *ACS Nano*, 2011, **5**, 5300-5311.
30. K. Kostarelos, *Nat Biotechnol*, 2008, **26**, 774-776.
31. K. Kostarelos, A. Bianco and M. Prato, *Nat Nanotechnol*, 2009, **4**, 627-633.
32. W. Wu, R. Li, X. Bian, Z. Zhu, D. Ding, X. Li, Z. Jia, X. Jiang and Y. Hu, *ACS Nano*, 2009, **3**, 2740-2750.
33. A. Battigelli, J. Russier, E. Venturelli, C. Fabbro, V. Petronilli, P. Bernardi, T. Da Ros, M. Prato and A. Bianco, *Nanoscale*, 2013, **5**, 9110-9117.
34. T. Omura, *J Biochem*, 1998, **123**, 1010-1016.
35. J. M. Worle-Knirsch, K. Pulskamp and H. F. Krug, *Nano Lett*, 2006, **6**, 1261-1268.
36. D. S. Youngblood, S. A. Hatlevig, J. N. Hassinger, P. L. Iversen and H. M. Moulton, *Bioconjugate Chem*, 2007, **18**, 50-60.
37. C. Samori, H. Ali-Boucetta, R. Sainz, C. Guo, F. M. Toma, C. Fabbro, T. da Ros, M. Prato, K. Kostarelos and A. Bianco, *Chem Commun (Camb)*, 2010, **46**, 1494-1496.
38. S. Varum, A. S. Rodrigues, M. B. Moura, O. Momcilovic, C. A. t. Easley, J. Ramalho-Santos, B. Van Houten and G. Schatten, *PLoS One*, 2011, **6**, e20914.
39. C. F. Chin, S. Q. Yap, J. Li, G. Pastorin and W. H. Ang, *Chem Sci*, 2014, **5**, 2265-2270.
40. S. Elmore, *Toxicol Pathol*, 2007, **35**, 495-516.
41. I. Vermes, C. Haanen, H. Steffens-Nakken and C. Reutelingsperger, *J Immunol Methods*, 1995, **184**, 39-51.
42. S. L. Yoong, B. S. Wong, Q. L. Zhou, C. F. Chin, J. Li, T. Venkatesan, H. K. Ho, V. Yu, W. H. Ang and G. Pastorin, *Biomaterials*, 2014, **35**, 748-759.
43. L. Wei, Y. Zhou, Q. Dai, C. Qiao, L. Zhao, H. Hui, N. Lu and Q. L. Guo, *Cell Death Dis*, 2013, **4**, e601. Available from URL: <http://www.ncbi.nlm.nih.gov/pubmed/23598413>.
44. N. Y. Fu, S. K. Sukumaran, S. Y. Kerk and V. C. Yu, *Mol Cell*, 2009, **33**, 15-29.
45. S. K. Sukumaran, N. Y. Fu, C. B. Tin, K. F. Wan, S. S. Lee and V. C. Yu, *Mol Cell*, 2010, **37**, 768-783.
46. N. Y. Fu, S. K. Sukumaran and V. C. Yu, *Proc Natl Acad Sci U S A*, 2007, **104**, 10051-10056.